Geol. Mag. **145** (*2*), *2008, pp. 279–294.* © *2008 Cambridge University Press*
doi:10.1017/S0016756807003998 First published online 25 January 2008 *Printed in the United Kingdom*

Depositional origin of tuffaceous units in the Pliocene Upper Siwalik Subgroup, Jammu (India), NW Himalaya

G. M. BHAT*, S. N. KUNDAL, S. K. PANDITA & G. V. R. PRASAD

Postgraduate Department of Geology, University of Jammu, Jammu – 180 006, India

(*Received* 14 November 2006; *accepted* 26 February 2007)

Abstract – During late Pliocene times, extrabasinally derived acidic volcanic ashes were deposited as distal pyroclastic fallout in upland interfluvial–lacustrine settings in the northwestern part of the Siwalik basin. These ash beds occur as a bentonitized tuff band and tuffaceous mudstones in the Jammu region of India. We located and described 12 outcrops of this conspicuous, geographically widespread bentonitized tuff band and tuffaceous mudstone association at the same stratigraphic level, coincident with the Gauss–Matuyama boundary at 2.48 Ma. This bentonitized tuff band and tuffaceous mudstone association represents a stratigraphic marker horizon in the diachronous and sporadic vertebrate fauna-yielding Siwalik strata. The claystone, siltstone, and sandstone units and embedded bentonitized tuff band and tuffaceous mudstone beds represent a coarsening-upward sequence reflecting deposition in lacustrine proximal and distal bottomsets, pro-delta foresets, and mouth-bar facies capped by fluvial topsets. This study reports a chain of four contemporaneous, palaeo-lake basins at this stratigraphic level, which ranged in length from 2 to 7 km.

Keywords: Siwalik, Jammu India, bentonitized tuff band, marker horizon, sandy debris flow, upland interfluvial–lacustrine sedimentation.

1. Introduction

In the Himalayan Foreland Basin, the Jammu region exhibits some spectacular exposures comprising a $\sim$6 km thick succession of Siwalik strata (Middle Miocene–Early Pleistocene). These diachronous strata are persistent for tens of kilometres along-strike in the region. The sporadic occurrence of megavertebrate fauna and the diachronous nature of the constituent strata pose problems in classifying these rocks into formal stratigraphic units. However, following the lithological similarities with their counterparts in the type sections in Pakistan, these strata have been traditionally classified as the Lower, Middle and Upper Siwalik subgroups. This terminology does not conform to the stratigraphic code of nomenclature but these terms are deeply engraved in literature and are being widely used. The Pliocene–Pleistocene stratigraphic record in the Northwest Himalaya documents a number of volcanic ash beds (bentonitized tuff bands and tuffaceous mudstones) at different stratigraphic levels. Earlier these beds were reported from Potwar Plateau (Burbank & Tahirkheli, 1985) and the Jhelum area (Johnson *et al.* 1982) in Pakistan, and from the Ghaggar and Khetpurali sections (Pinjore Formation) near Chandigarh in India (Tandon & Kumar, 1984) (Fig. 1). Ranga Rao *et al.* (1988) reported their occurrence in the Upper Siwalik Subgroup at Jammu from three localities: Bali, Nagrota and Bada Khetar. Ranga Rao *et al.* (1988) and Gupta & Verma (1988) have proposed different stratigraphic classifications for the Upper Siwalik Subgroup of Jammu. Although both classifications conform to the code of stratigraphic nomenclature, we followed the classification of Ranga Rao *et al.* (1988) in view of its priority and wide usage. This classification proposes subdivisions of Upper Siwalik Subgroup into Purmandal Sandstone (= Purmandal Formation), Nagrota Formation and Boulder Conglomerate Formation. Demarcation of the formational boundaries is based on megavertebrate fauna, palaeomagnetic data and fission track dates of zircon phenocrysts recovered from the embedded bentonitized tuff band (Ranga Rao *et al.* 1988). The basal part of the Nagrota Formation is dominantly composed of alternating claystone, siltstone and sandstone facies, which grade into alternation of siltstones, claystones and sandstones with pebble bed intercalations towards the top. Agarwal *et al.* (1993) informally divided the Nagrota Formation into Nagrota A, Nagrota B and Nagrota C members (Fig. 1) on the basis of their bio-magnetostratigraphic studies and analysis of satellite images, together with measurement of ground spectral signatures of various rock units in the area north of Samba town. The bentonitized tuff band and tuffaceous mudstones occur towards the top of the Nagrota B Member. Although known at three localities (Bada Khetar, Nagrota and Bali at the same stratigraphic level) for the last few decades, no information is available on persistence, depositional processes and mode of preservation of this bentonitized tuff band and tuffaceous mudstones. We located and measured them in ten additional localities at the same

*Author for correspondence: bhatgm1@rediffmail.com

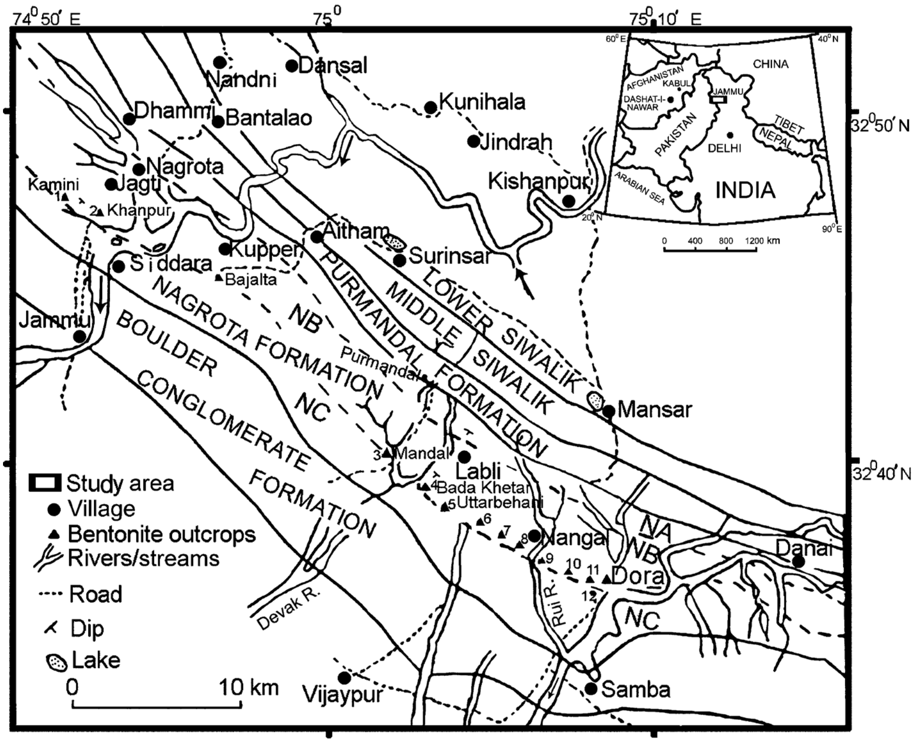

Figure 1. Geological map of the Siwalik Group at Jammu and location of outcrops of bentonitized tuff band. NA – Nagrota A Member, NB – Nagrota B Member, NC – Nagrota C Member. Inset regional map showing location of bentonitized tuff band in Pakistan (Potwar plateau) and India (Jammu and Chandigarh). Stratotype Dashat-i-Nawar volcanic complex, Afghanistan, is also shown.

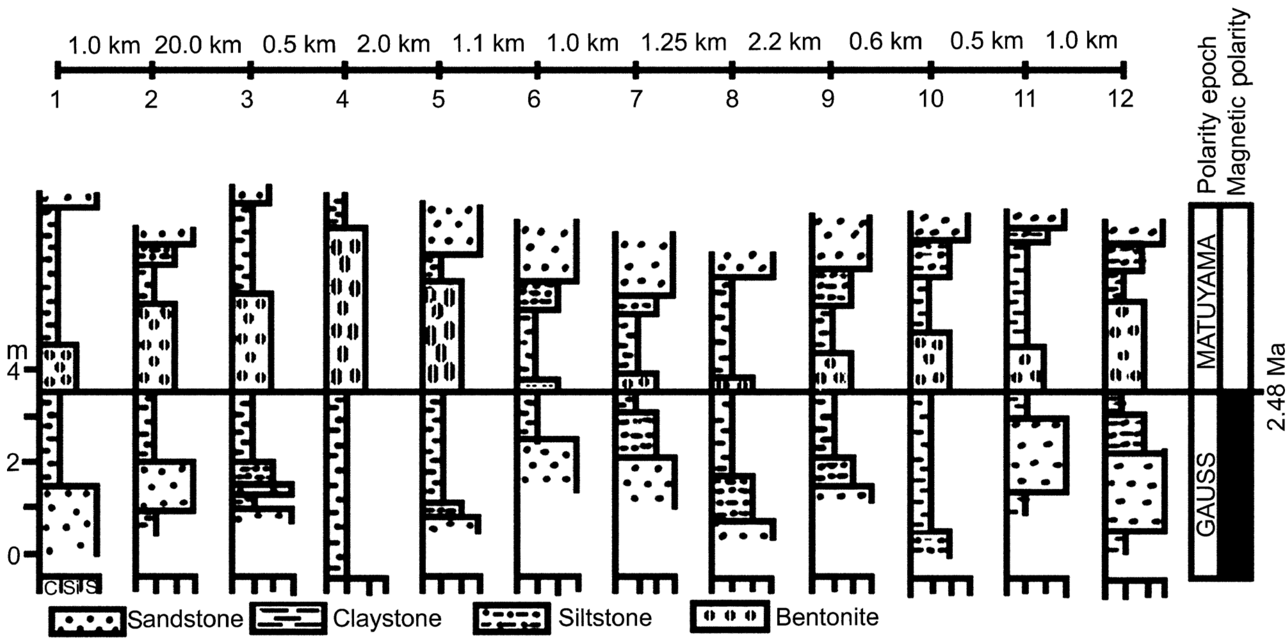

Figure 2. Lithologs of the 12 stratigraphic sections containing bentonitized tuff and tuffaceous mudstone beds in the study area. The sections measured include: 1 – Kamini, 2 – Khanpur, 3 – Mandal, 4 – Bada Khetar, 5 – Uttar Behani, 6 – Anandpur *nala*, 7 – Stony Waste, 8 – Kherdi, 9 – Teri, 10 – Karju *Tiba*, 11 – Karju *nala*, 12 – Dora.

stratigraphic level in the region (Fig. 1); the measured sections are shown in Figure 2. The volcanic ash falls are short-lived events, and represent unique chronostratigraphic index horizons, being for all practical purposes geological time planes. The bentonitized tuff band and tuffaceous mudstones of this study represent one of these event-stratigraphic units, which are rarely preserved in the geological record, particularly in the continental strata. We focused on this conspicuous and geographically widespread bentonitized tuff band, the tuffaceous mudstones and the associated strata to decipher their depositional origin.

2. Field observations

During our detailed field study in the 7 km stretch from Tawi River to Tanda *nala* (northwestern part of the project area; *nala*, small rain-fed stream) and the 12 km stretch from Mandal to Dora villages (southeastern part of the project area), we located and traced the continuity of the bentonitized tuff band and tuffaceous mudstone beds in 12 detached but closely spaced outcrops over a total distance of about 45 km along-strike. Out of these 12 outcrops, the Kamini (1) and Khanpur (2) sections occur between the Tanda *nala* and Tawi River in the northwestern part of the study area; the next three sections (Mandal (3), Bada Khetar (4) and Uttar Behani (5)) occur between the Devak River and Labli *nala*; the next three (Anandpur (6), Stony Waste (7) and Kherdi (8)) occur between the Labli *nala* and Rui River; and the last four (Teri (9), Karju *Tiba* (small hillock) (10), Karju *nala* (11) and Dora (12)) occur between the Rui and Basantar rivers in the southeastern part of the study area (Fig. 1). The Kamini section occurs in the Kamini *nala* southwest of Nagrota. The bentonitized tuff band and tuffaceous mudstone beds are traceable on either side of the Kamini *nala* across the two hillocks for about 1 km. We traced their continuity further for about 3 km in the northwest direction up to the Tanda *nala* in detached outcrops. The Khanpur section occurs about 1 km southeast of the Kamini section. This section is exposed on the Nagrota bypass road in a hillock and can be traced on one side of the road for about 1.5 km along-strike up to the right bank of the Tawi River. On the other side its continuity can be traced out across the hillock in the Kamini *nala*. So far, we have located the bentonitized tuff band and tuffaceous mudstones in the stretch between the Tawi River and Tanda *nala* for about 7 km in the strike continuation. There is evidence of the occurrence of this bentonitized tuff band and the tuffaceous mudstone beds in the strike continuation from Khanpur village near Nagrota up to Mandal for a distance of about 20 km (Fig. 1). In this stretch, recently we located another outcrop across the Tawi River near Bajalta village on the Jammu–Surinsar road; our work is in progress in this area. The Mandal section occurs on the link road between Mandal and Bada Khetar villages at a distance of about 0.5 km from Bada Khetar. The Bada Khetar section is exposed in the hillock at Bada Khetar village. The 3.6 m thick bentonitized tuff band exposed at this locality is the thickest known in the entire Himalayan Foreland Basin (Bhat *et al.* 1999); it laterally pinches out to 2.8 m within a few hundred metres (Fig. 3). The Uttar Behani section occurs about 2.0 km southeast of the Bada Khetar section at about 1 km north of Uttar Behani village. The main Uttar Behani section occurs in a hillock situated on the left bank of the Devak River (Fig. 1). Northwest from Uttar Behani

Figure 3. Bentonitized tuff band, exposed at Bada Khetar (2.65 m) where it acquires maximum thickness (3.6 m), overlying brownish mudstone beds.

to Bada Khetar village, a number of eroded bentonitized tuff and tuffaceous mudstone beds are exposed in the dislocated hillocks and *nala* cuts. All these bentonitized tuff and tuffaceous mudstone beds are in the strike continuation for a distance of about 2 km and occur at the same stratigraphic level through out the area. The bedding has become so obscure due to dislocation and erosion that none of these exposures is worth measurement and description. The Anandpur section occurs in the Labli *nala* about 1 km from Anandpur village. The Stony Waste section occurs to the southeast, on the top of the hillock in the strike continuation of the Anandpur section. Between Nangal and Kherdi villages, a number of eroded bentonitized tuff and tuffaceous mudstone beds are observed in low-lying hillocks and *nala* cuts. All of these remnant beds were traced in the same strike direction and at the same stratigraphic level covering an area of about 5 km^2 and are embedded in similar claystone units in all the outcrops. However, none of these exposures could be measured or described due to their dislocation and erosion. The main Kherdi section lies northwest of Kherdi village at a distance of about 0.875 km. At Teri (Bardan hutment), near Nangal village, the bentonitized tuff band is exposed in the road-cut section, whose continuity is traced across the tableland in the Rui River section. This section is about 1.375 km south of Nangal village (Fig. 1) and occurs in the strike continuation of the Karju *Tiba* section. The Karju *nala* outcrop occurs about 1 km to the northwest of the Dora section, which is exposed at the base of a hillock about 0.62 km northwest of Dora village. The extension of this outcrop is seen in a *nala* section just on the other side of this hillock.

The bentonitized tuff band and tuffaceous mudstones are bounded by brownish claystones and siltstones, which yield diverse types of microfossils (rodents, lizards, fishes, ostracodes, gastropods, etc.) and microflora (charophytes, angiosperm seeds, etc.). Occasionally, grey sandstone and tuffaceous mudstone intercalations are present within the bentonitized tuff

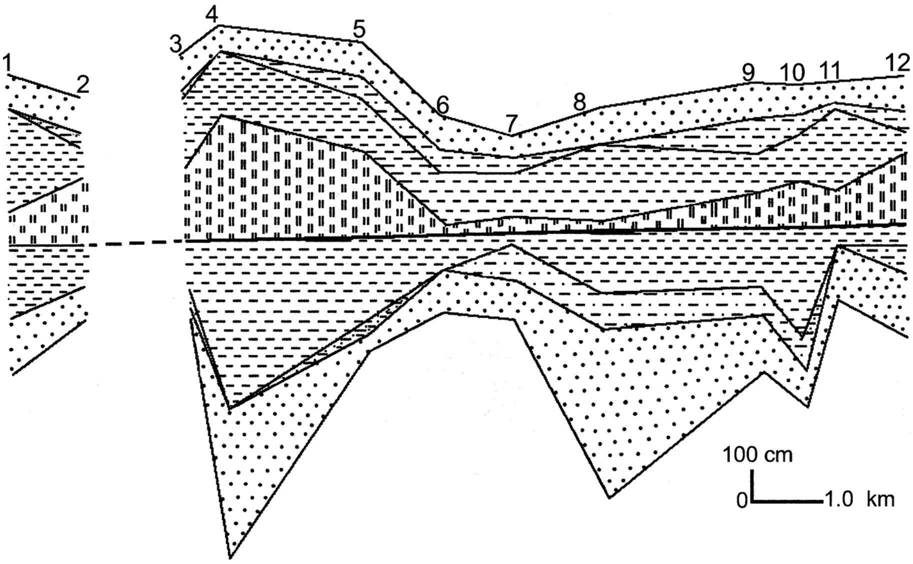

Figure 4. Spatio-temporal lithofacies architecture of the bentonitized tuff, tuffaceous mudstone and associated strata in the 12 measured sections. For locality names and explanation of lithofacies symbols, refer to Figure 2.

band, which is mainly composed of two types of sediments: (1) cream- and pink-coloured bentonite having a high swelling property, and (2) white-coloured, powdery and sandy bentonite clay having little swelling character. The tuffaceous mudstones occur at the base of the bentonitized tuff band in the Kamini, Khanpur, Uttar Behani, Teri, Karju *nala*, Karju *Tiba* and Dora sections, while in the Stony Waste and Kherdi sections the mudstones occur on top. The bentonitized tuff band is internally composed of many subunits and exhibits graded bedding, planar and wavy lamination, cross-lamination, load and flame structures, convolute bedding, oscillation ripples, bioturbation, pinch and swell structures, and escape burrows (both vertical and inclined). The bentonitic clay unit contains mudstone pebbles. Generally, all of the bentonitized tuff beds show subtle variation in grain size and colour (pinkish to cream).

In all 12 measured sections the strata can be divided into three lithounits: the strata underlying the bentonitized tuff band and tuffaceous mudstones (lithounit 1), bentonitized tuff band and tuffaceous mudstones (lithounit 2) and the strata overlying the bentonitized tuff band and tuffaceous mudstones (lithounit 3). The bentonitized tuff band is generally composed of grains 4–6 phi in size. However, in some of the measured sections a few beds are composed of bentonitized tuff beds (Tawi River section) whose grain size ranges from 1 to 4 phi. The tuffaceous mudstone beds are commonly represented by grey to dark grey and olive claystones and sandy siltstones rich in biotite and hornblende, characteristic of most of the tuffaceous mudstone beds in the Siwalik strata (e.g. Johnson *et al.* 1982), and exhibit sharp basal contact with the claystones in the measured sections. The upper contacts of the bentonitized tuff band and tuffaceous mudstones with the claystone units are generally gradational in the measured sections. The bentonitized tuff band and tuffaceous mudstones yield platy and pumice-type glass shards, quartz and zircon phenocrysts, feldspar, hornblende, biotite and sanidine. The dominant clay mineral identified in the bentonitized tuff band is montmorillonite. The ferromagnesian minerals with specific gravity ranging from 3.1 to 4.7, and felsic minerals with specific gravity ranging from 2.5 to 2.6, form the dense and light layers, respectively, in the bentonitized tuff band and tuffaceous mudstone beds. Compositionally these bentonitized tuff beds are andesitic (dark coloured) and trachytic (light grey and olive) in nature (Bhat & Pandita, 1998). The spatio-temporal lithofacies architecture of the bentonitized tuff band, tuffaceous mudstones and associated strata in the 12 measured sections is given in Figure 4.

2.a. Lithofacies

We recorded five broad lithofacies, including sandstone, pebbly sandstone, siltstone, claystone and bentonite facies. These five broad facies are composed of 14 subfacies. The sandstone facies is composed of two subfacies, that is, sandstone and nodular sandstone. The siltstone facies is composed of two subfacies: siltstone and sandy siltstone. The claystone facies is composed of four subfacies including laminated claystone, sandy claystone, nodular claystone and claystone. The bentonite facies is composed of five subfacies including tuffaceous mudstone, nodular bentonite, sandy bentonite, clayey bentonite and pure bentonite. The claystone, siltstone, and sandstone facies are common in lithounits 1 and 3, while the nodular and sandy claystone facies and nodular sandstone facies are confined to lithounit 1 only. The pebbly sandstone and sandy siltstone facies

https://doi.org/10.1017/S0016756807003998 Published online by Cambridge University Press

Table 1. Relative percentages of various lithofacies recorded in the 12 measured sections

Facies	1	2	3	4	5	6	7	8	9	10	11	12
Pebbly sandstone	15	12	5	–	–	44	16	–	14	–	–	9
Sandstone	10	14	4	30	8	7	20	35	19	15	23	21
Nodular sandstone	–	4	–	24	–	–	–	15	–	–	–	–
Siltstone	–	18	–	11	8	8	24	11	24	6	16	19
Sandy silt	5	–	9	–	–	–	–	–	–	11	11	–
Claystone	40	24	33	14	14	24	26	29	29	47	13	25
Nodular claystone	–	–	7	–	5	–	–	2	–	–	–	–
Sandy claystone	–	8	3	–	8	–	–	–	–	–	–	–
Laminated claystone	12	5	9	4	11	–	–	8	–	7	12	5
Pure bentonite	–	–	–	1	38	5	–	1	–	–	3	3
Sandy bentonite	13	9	18	8	–	–	–	–	10	1	9	–
Nodular bentonite	4	2	5	5	–	7	3	–	2	11	7	–
Clayey bentonite	–	3	7	3	3	5	–	–	–	–	–	–
Tuffaceous mudstone	1	1	–	–	5	5	13	2	2	2	6	18

Localities: 1 – Kamini, 2 – Khanpur, 3 – Mandal, 4 – Bada Khetar, 5 – Uttar Behani, 6 – Anandpur *nala*, 7 – Stony Waste, 8 – Kherdi, 9 – Teri, 10 – Karju *Tiba*, 11 – Karju *nala*, 12 – Dora.

are restricted to lithounit 3. The relative percentages of these 14 lithofacies are given in Table 1. The sandstone facies ranges from 4 % in the Mandal section to 54 % in the Bada Khetar section. The pebbly sandstone facies constitutes 5 % in the Mandal section and 44 % in the Anandpur section, while the claystone facies ranges from 14 % in the Bada Khetar section to 54 % in the Karju *Tiba* section. The siltstone facies ranges from 11 % in Bada Khetar and Kherdi sections to 27 % in Karju *nala* section. The bentonite and tuffaceous mudstones are dominant in the Uttar Behani section (46 %) and minimal in the Kherdi section (3 %).

2.a.1. Sandstones

2.a.1.a. Sandstone facies (Sst-facies) The Sst-facies varies in thickness from 51 to 320 cm and is present in the basal lithounit 1 of sections 1, 2, 4 and 7–12. This facies is also present in lithounit 3 in the sections 1, 4, 5, 8, 10 and 12. The Sst-facies is mainly composed of grey to light grey, compact (sections 1–11) and friable (section 12) sandstones. The base of the sandstone facies is coarse grained, followed upward by medium- to fine-grained sandstones (sections 1, 4, 5, 10, 11). In some of the measured sections (7, 8, 9, 10), the Sst-facies is composed of coarse- and fine-grained, cross- and wavy-laminated sandstone couplets in which the coarse-grained units are cross-bedded and the fine-grained ones are laminated. In some of these and in other cases the top of the facies is characterized by patches of clay lenses (sections 2, 8) and ripple lamination (section 9). In sections 3, 4, 11 and 12, the top of the Sst-facies is represented by reverse-graded medium- to coarse-grained sandstone units which exhibit cross-bedding and ripple lamination. In lithounit 3, the Sst-facies is more or less similar in character to the Sst-facies in lithounit 1. In section 3 this facies is composed of dark grey reverse-graded friable sandstone with scoured base and laminated top. The top of section 3 is marked by a 20 cm thick, reddish brown silty sandstone unit. Generally this facies in lithounit 3 is normal graded. The basal part is composed of grey, coarse-grained sandstone and is followed upward by light grey, fine-grained sandstones (sections 2, 4, 5, 6, 8, 9, 10, 12). These sandstones are characterized by patches of clay lenses and lamination (sections 4, 5, 8, 10, 12). In sections 4 and 12 this facies exhibits cross- and wavy lamination.

2.a.1.b. Nodular sandstone facies (NSst-facies) The NSst-facies is present in only three sections (2, 4, 8). The base of this facies is represented by a thin layer of coarse-grained sandstones. This layer shows pinch and swell structures. Above this unit is a fine-grained light grey sandstone unit showing load structures, followed upward by a grey coarse-grained sandstone unit. The overlying fine-grained sandstone unit is ripple and wavy laminated. Overall the NSst-facies is dominated by ripple marks and alternation of sandstone nodules and grey claystone lenses. The nodules are composed of coarse-grained sandstone whose size is the same throughout the section.

2.a.2. Pebbly sandstone facies (PSst-facies)

The PSst-facies occurs in seven measured sections (1, 2, 3, 6, 7, 9, 12) and only in lithounit 3. This facies is composed of 36–100 cm thick sandstone beds containing silt/clay intercalations and pebbles. The facies is generally reverse-graded with an imbricated pebble layer at its top. Thin layers of compact reddish to light brown siltstone/clay occur within this facies (sections 1, 6, 7, 9, 12). The sandstone layers exhibit symmetrical ripples having sharp crests and rounded troughs (sections 1, 7, 12). This facies shows an erosional/scoured upper contact (sections 1, 2). The base of the PSst-facies is represented by dark grey (sections 2, 7, 9), brownish (section 6), coarse-grained sandstone containing light grey, fine-grained sandstones and pebbles (sections 4, 6) and is cross- and wavy laminated (sections 6, 9). The facies is composed of fine- to coarse-grained friable pebble-bearing sandstones with interbedded clay pebbles in section 12, whose top is marked by a coarse-grained sandstone unit, which normally grades upward into fine-grained sandstone.

2.a.3. Siltstones

2.a.3.a. Siltstone facies (Si-facies) The Si-facies is composed of reddish-brown laminated siltstone whose

https://doi.org/10.1017/S0016756807003998 Published online by Cambridge University Press

thickness varies from 20 to 150 cm in lithounit 1 (sections 5, 8–12) and from 28 to 100 cm in lithounit 3 (sections 2, 5, 6, 7, 12). This facies is generally laminated and sometimes structureless, and pinches out laterally. In some cases the top of the Si-facies is draped by light grey rippled sandstone facies (section 4, lithounit 1 and sections 5, 6, 8 and 11, lithounit 3) and in others is subtly normal graded (section 5, lithounit 1), showing subtle variation in grain-size and colour (section 2, lithounit 1). The basal contacts of the Si-facies with the underlying sandstone facies (section 12, lithounit 1) and claystone facies (section 12, lithounit 3 and section 10, lithounit 3) are gradational.

2.a.3.b. Sandy siltstone facies (SSi-facies) The Ssi-facies is composed of alternating light grey and reddish fine-grained sandstones and siltstones. The thickness of this facies varies from 48 to 100 cm. In some cases, the Ssi-facies exhibits pebble layers and shows variation in colour from bottom (reddish brown) to top (light grey) (sections 1, 11). In section 3 this facies exhibits mud pebbles in sandstone layers while the sandstone layers exhibit symmetrical ripples in section 10. The sandy units of the Ssi-facies show normal grading (Section 11).

2.a.4. Claystone facies

2.a.4.a. Laminated claystone facies (Lc-facies) The Lc-facies is composed of brownish and light grey claystones in lithounit 1 (sections 1–4, 8, 10–12) and brownish (sections 1, 2, 5, 10–12) and light grey (sections 3, 4) claystones in lithounit 3. Thickness of this facies varies from 45 to 150 cm in lithounit 1 and from 34 to 200 cm in lithounit 3. The finely laminated claystone beds are hard and compact, having a maximum thickness of 45 cm. The claystone units are fossiliferous and yield rodent molars, lizards, fishes, fragmentary bones of microvertebrates, and microfauna including ostracodes, gastropods and microflora (charophytes). The Lc-facies generally shows sharp basal contact with the bentonite facies and a gradational top, except in sections 1 and 10 where the facies shows sharp contact with the overlying tuffaceous mudstone facies. In section 10 the Lc-facies exhibits gradational contact with the underlying sandy bentonite facies.

2.a.4.b. Sandy claystone facies (Sc-facies) The Sc-facies is composed of grey sandstone and light grey–brown claystone couplets whose thickness varies from 30 cm (section 5) to 150 cm (section 2). The sandstone beds are normal graded and the claystone units are laminated. The contact between the sandstone and claystone units is subtly gradational. The fossiliferous coarse-grained sandy layers exhibit well-preserved symmetrical ripples on their tops (section 5). The basal contact of this facies is sharp with the underlying B-facies, and the top exhibits gradational contact with the overlying silt facies of lithounit 1 (section 3).

2.a.4.c. Nodular claystone facies (Nc-facies) The Nc-facies is composed of grey claystone whose thickness varies from 25 to 150 cm. This facies occurs in lithounit 1 (sections 5, 8) and in lithounit 3 (section 3). The Nc-facies is finely laminated at its top. The nodules show normal grading and vary in diameter from 2 to 3 cm.

2.a.4.d. Claystone facies (Cs-facies) The claystone facies is composed of brownish and grey, structureless claystone whose thickness varies from 21 to 100 cm in lithounit 1 and from 23 to 250 cm in lithounit 3. The brownish claystone units of this facies are fossiliferous and yield microvertebrates including rodent molars, lizards, frogs, and microfauna including ostracodes, gastropods, charophytes and angiosperms (sections 4, 5, 6, 12). This facies pinches out laterally and shows sharp contact with the bentonite facies (sections 5, 6) and tuffaceous mudstone facies (section 9). The Cs-facies yields gastropods and ostracodes (section 6, 8) and fragmentary bones of microvertebrates and charophytes (section 9) in lithounit 3. The top of this facies is marked by sharp-crested rippled fine-grained sandstone layers (section 10) in lithounit 3.

2.a.5. Bentonite facies

2.a.5.a. Tuffaceous mudstone facies (Tm-facies) The Tm-facies occurs in ten of the measured sections (1, 2, 5–12). The thickness of this facies varies from 6 cm (section 1) to 32 cm (section 6). Generally, the Tm-facies is composed of dark grey and greenish (section 12), greasy/soapy tuffaceous mudstone. It contains quartz, feldspars, zircon, apatite, hornblende, biotite, etc. The facies shows pinch and swell structures in all of the measured sections and exhibits sharp basal contact with the underlying claystone facies (sections 1, 2, 5, 6, 8–11) or bentonite facies (sections 7, 12). It has a sharp contact with the overlying claystone facies (sections 6, 8) or bentonite facies (sections 1, 2, 5, 9–12). In section 7, the Tm-facies exhibits gradational contact with the overlying claystone facies. The Tm-facies is soft and greasy when soaked in water and becomes tough and friable when dry. It shows wavy lamination in section 9, and wavy and cross-lamination in sections 10, 11 and 12.

2.a.5.b. Nodular bentonite facies (Nb-facies) The Nb-facies is composed of pinkish, cream and white nodular bentonite (sections 1, 2, 3, 4, 7, 9, 10, 11). Its thickness varies from 6 cm (section 7) to 103 cm (section 10). The diameter of the nodules ranges from 1.2 to 4 cm. The nodules show reverse size grading in some sections (sections 4, 11). The Nb-facies shows a sharp basal contact with the underlying claystone facies (section 7). In section 1 a layer of fine-grained grey sandstone occurs at its top. Internally the Nb-facies is composed of nodular and wavy-laminated units (sections 6, 10) and shows colour variation from pinkish to white. Some of the units of this facies contain escape burrows

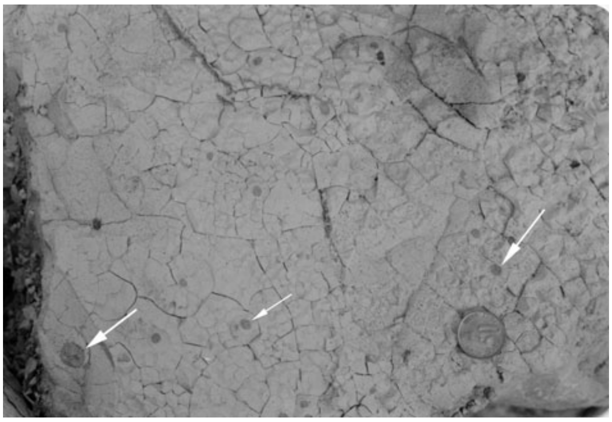

Figure 5. Field photograph of nodular bentonite showing liquefaction features (arrows), Bada Khetar section. The grey circular patches on the bentonite layer are composed of fine sandstone ejected from the underlying fine sandstone layer of the same colour and composition (diameter of the coin is 23 mm).

(sections 10, 11) and have clay lenses (section 11). A few beds exhibit small-scale liquefaction features (Fig. 5). Laterally the facies shows a pinch and swell character. In section 4 the Nb-facies exhibits a sharp contact with the overlying microfossil-yielding claystone facies, while in section 9 the Nb-facies exhibits a gradational contact with the overlying claystone facies of lithounit 3.

2.a.5.c. Sandy bentonite facies (Sb-facies) The Sb-facies is composed of grey to off-white, fine-grained sandy bentonite and occurs in sections 1–4 and 9–11. The thickness of this facies varies from 12 cm (section 1) to 130 cm (section 2). The intervening fine-grained sand layers are laminated and rippled, and exhibit brownish clay lenses and escape burrows (sections 2, 4, 9). In some cases the intervening medium- to coarse-grained sand layers display cross-bedding and wave ripples (sections 3, 4, 9). This facies is subtly normal graded, and the beds pinch out laterally. Over this unit lies a 25 cm thick sandy bentonite bed in which small pure bentonite nodules occur. In some cases, mud pebbles occur within the Sb-facies (sections 4, 11). The top of this facies is generally represented by a wavy-laminated bentonite unit (section 3, 4, 9) and exhibits a gradational contact with the overlying claystone facies of lithounit 3 (sections 2, 10, 11). This facies is characterized by load and flame structures (section 2) (Fig. 6) and graded, laminated, rippled (Fig. 7) and cross-bedded units (section 2). The basal contact of this facies is generally sharp with the underlying claystone or bentonite facies and with the Tm-facies (section 9). The Sb-facies is generally friable and has less swelling character.

2.a.5.d. Pure bentonite facies (B-facies) The B-facies occurs in only six sections (4, 5, 6, 8, 11, 12). This facies is composed of pinkish and creamish bentonite units which are highly swelling in nature. The bentonite

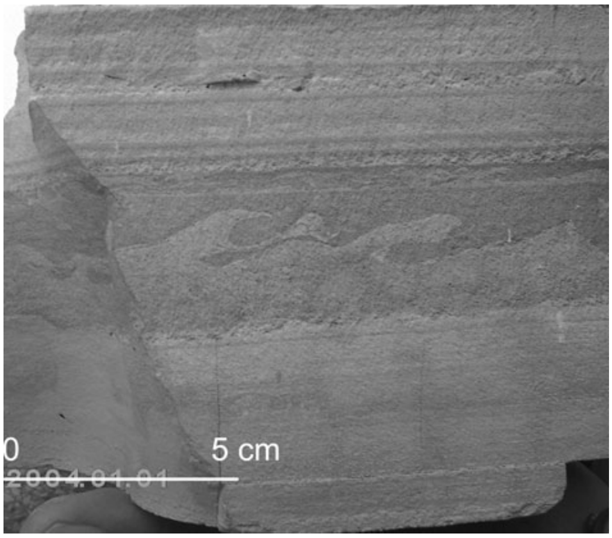

Figure 6. Photograph showing dark and white couplets of andesitic and felsic ash layers documenting different episodes of eruption of magma chamber and displaying load and flame structures, also see the variation in bed/lamina thickness (Tawi River section).

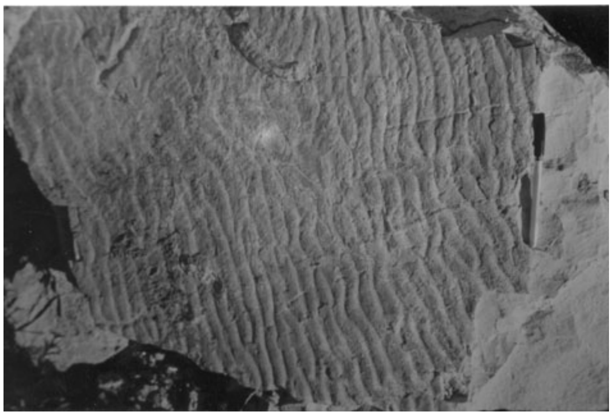

Figure 7. Photograph showing tuning fork-type wave ripples in a bentonitized tuff band, Bada Khetar outcrop (length of pen = 15 cm.).

has a plastic, greasy and soapy character. Its thickness varies from 6 cm (section 4) to 30 cm (section 12) and it exhibits pinch and swell structures. The facies occurs at the base of the measured sections and shows sharp contact with the underlying claystone units. When soaked in water it becomes pinkish in colour. The dry samples of this facies give a soapy feel and are brittle, having conchoidal-like fractures. In section 5 it has a sharp contact with the underlying Tm-facies.

2.a.5.e. Clayey bentonite facies (Cb-facies) The Cb-facies is composed of off-white to light grey, very soft bentonite beds which occur in five sections (2–6) and vary in thickness from 6 cm (section 6) to 100 cm (section 4). These beds show pinch and swell structures. This facies is generally structureless and friable. In some cases it contains mud pebbles and clay lenses which are a few centimetres to a few metres in

https://doi.org/10.1017/S0016756807003998 Published online by Cambridge University Press

length (sections 3, 4, 5). The clay lenses are internally laminated. Both vertical and inclined escape burrows are prevalent in this facies. The Cb-facies exhibits gradational contact with the overlying claystone facies (section 5).

2.b. Depositional facies and interpretation

The Nagrota Formation is composed of a number of vertical and lateral stacks of interfluvial sequences. One of these sequences embedding the bentonitized tuff band and tuffaceous mudstone beds towards the top of Nagrota B Member is composed of vertically and laterally varying facies architecture and represents fluvial–lacustrine settings (Fig. 8). This sequence typically shows distinct coarsening-upward facies stacks ranging from silty, wavy bottomsets to sandy prodelta foresets with overlying mouth-bar facies capped by fluvial sandstone and gravel beds (Fig. 9). The stratigraphic sections measured between Dora and Karju Tiba, Kherdi and Anandpur, Uttar Behani and Mandal, and Khanpur and Kamini exhibit four such sequences, in which the bentonitized tuff band and tuffaceous mudstone beds are embedded. However, there are minor variations in facies stacks among the measured sequences. These four facies sequences reflect deposition in four different coeval lakes. These palaeo-lakes were spread over 2 to 7 km. Among these four lake basins, the Uttar Behani–Mandal (spread over more than 3 km) and Khanpur–Kamini (spread over about 7 km) areas exhibit the record of well-preserved facies stacks representing typical lacustrine depositional settings. The delta foreslope outside the channels represents muddy sediments, and the central plain records thinly bedded claystones and siltstones, which embed the bentonitized tuff band, tuffaceous mudstones and thin sandstone layers. Description of the main facies sequences representing the different depositional interfluvial–lacustrine settings follows.

2.b.1. Primary lacustrine facies

2.b.1.a. Direct settling of ash-fall facies Rhythmites are sequences of finely laminated, regular alternations of two or more contrasting sediment types. They probably represent the most characteristic lacustrine facies and occur as horizontal, millimetre- to sub-millimetre-thick laminae (laminites). Varves are the best known rhythmites and comprise couplets of clastic sediments which differ in colour and texture, but all rhythmites are not varves. Rhythmites composed of two sediment types in the bentonitized tuff band are remarkably laterally persistent and can be traced for hundreds of metres with no change in thickness or grain size. Coarse-grained laminae are mostly thicker than the fine-grained laminae. Most of the laminae show sharp bases. We also observed occasional rhythmic patterns on a millimetric scale, displaying

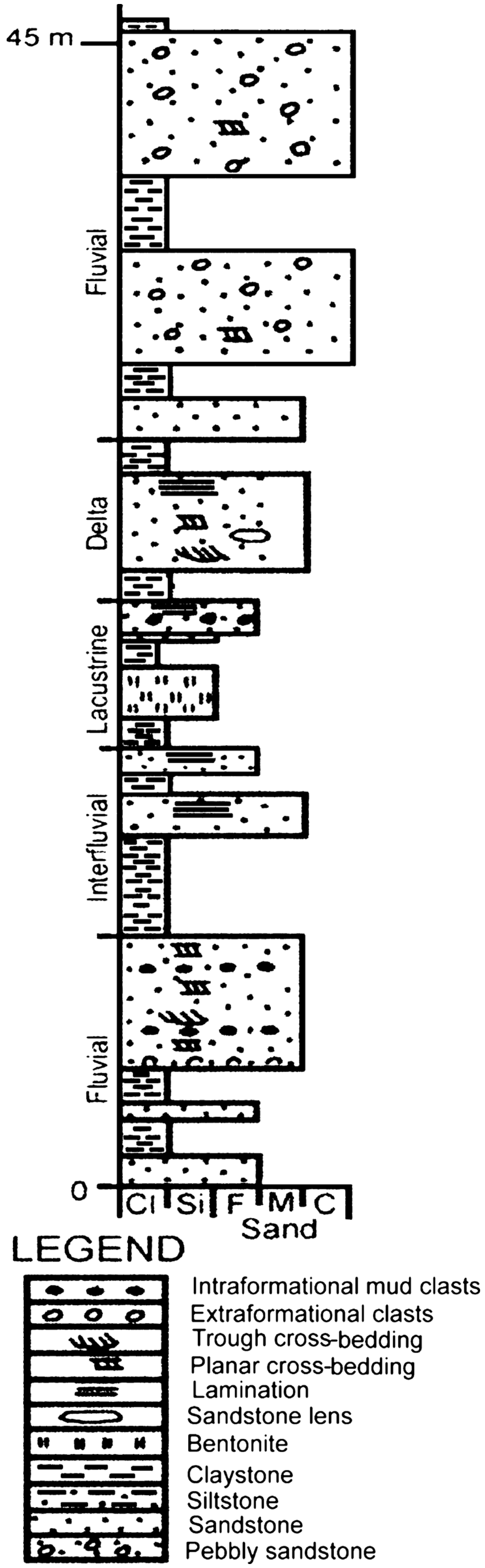

Figure 8. Litholog of the succession exposed at Khanpur displaying different depositional stacks.

https://doi.org/10.1017/S0016756807003998 Published online by Cambridge University Press

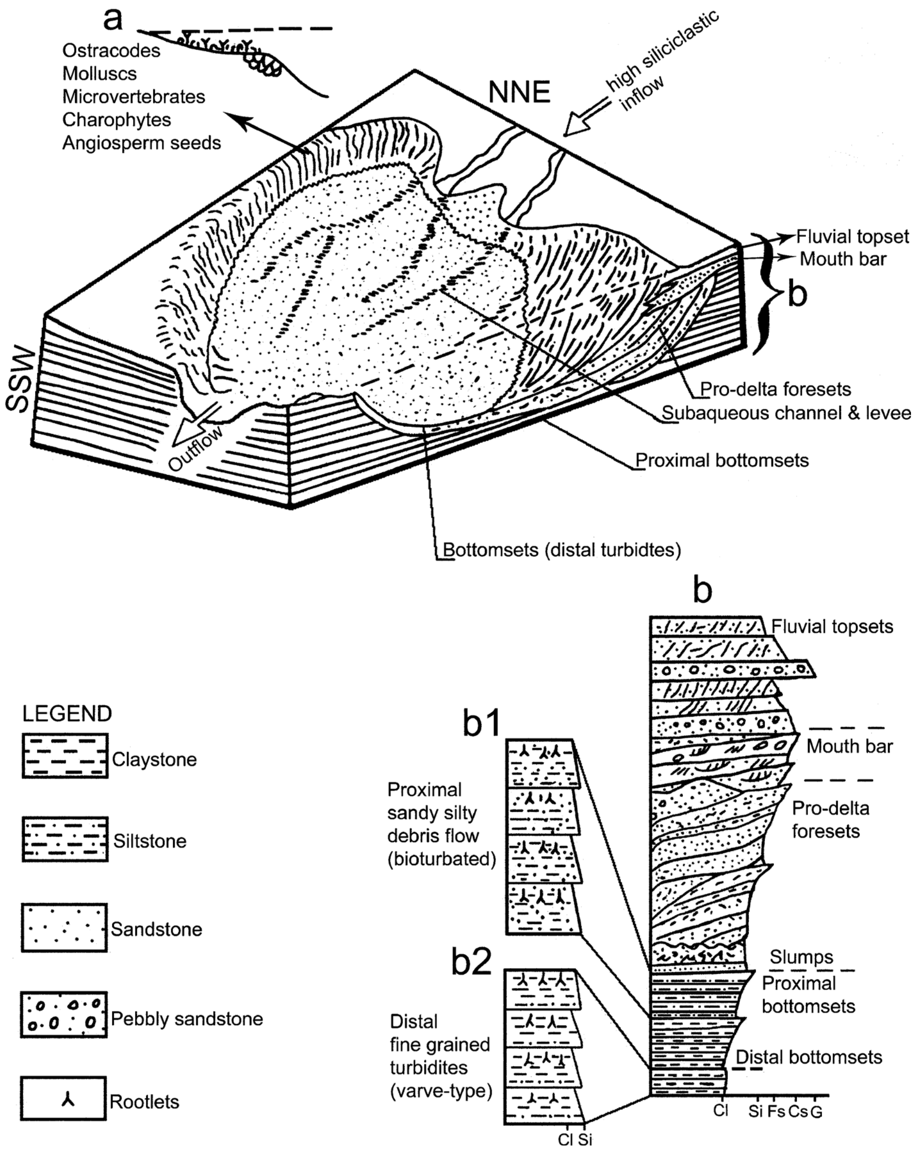

Figure 9. Depositional model of bentonitized tuff, tuffaceous mudstone and associated beds in upland interfluvial–lacustrine conditions. (a) Lake shore which is little influenced by river inflow and receives little sediment (fine-grained) from the upland region during the rainy season, providing sustainable conditions for floral growth. (b) Idealized sequence of distant and proximal bottomsets, pro-delta foresets, mouth-bar and fluvial topsets.

stratification composed of a succession of discrete layers of tuff (Fig. 6). Moreover, laminae are mutually grouped into laminae-sets. These laminae-sets include predominantly fine- and coarse-grained tuffs, and successive graded packages. This facies architecture suggests settling of size- and density-graded ash through the calm water column. The 11 cm thick dark and light-coloured tuff bed observed in the Tawi River bed (extension of the Khanpur section) exhibits 15 prominent divisions, including internally finely laminated planar, wavy and cross-lamination, convolute lamination, normal and reverse grading, structureless bedding, and load and flame structures (Figs 6, 10). The basal three units of this sequence are composed of a graded unit, parallel-laminated unit and wavy-laminated unit. These three units are related to suspension sediment settling, current-induced sediment reworking and waning stages of the current, respectively. In a similarly situated bentonitized tuff band, Johnson *et al.* (1982) reported small-scale cross-bedding and horizontal lamination from the uppermost 20 cm of the altered tuffaceous mudstone bed at Rhotash Anticline (Pakistan) and concluded that tuff was emplaced in lacustrine conditions. The laminae-sets in some bentonitized tuff beds (Tawi River section) show thickness variation in the couplets of light and dark layers. This variation in thickness of the couplets reflects variation in the rate and composition of ash fall on the lake surface (e.g. Sturm & Matter, 1978), as some ash falls are composite and consist of subunits that represent pulses within a single eruption event. Beds more than 10 cm thick show subtle

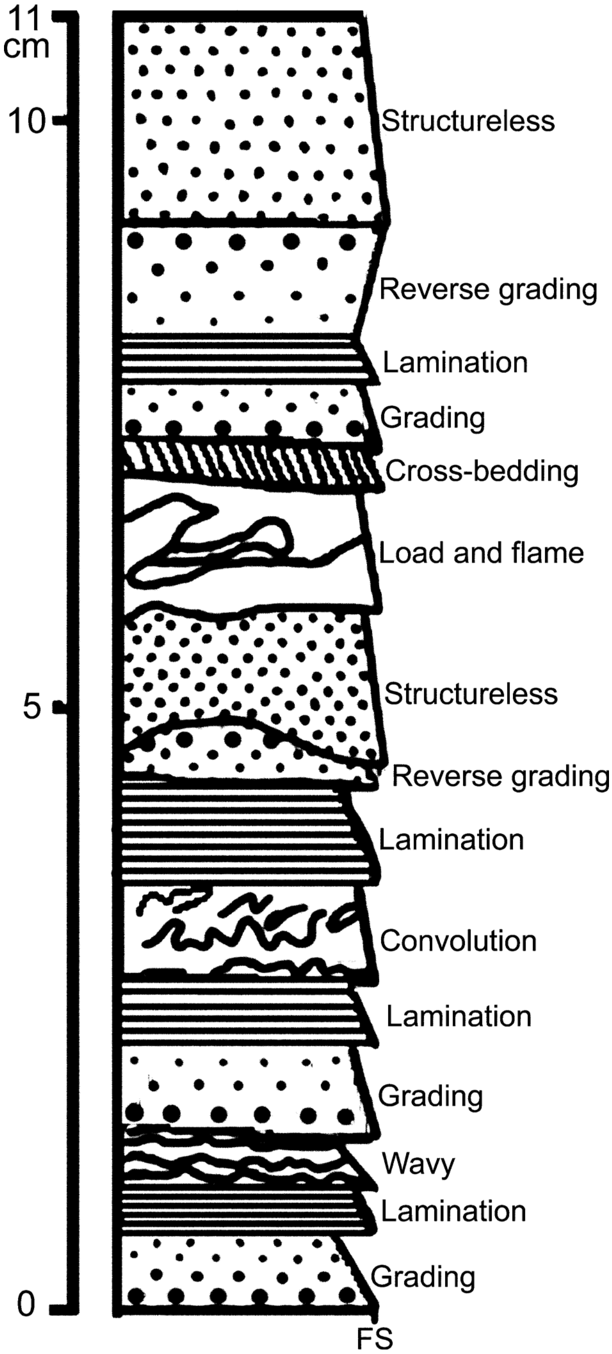

Figure 10. Sketch of an actual bentonite bed recorded in the Tawi River of Khanpur section representing 15 distinct units (FS – fine sand).

variation in grain size and sorting and exhibit diffuse internal stratification (e.g. Fisher & Schmincke, 1984). Interbedded thin fine-grained sandstone and siltstone layers are laminated and wavy in nature. By examining polished slabs and by logging the entire thickness of the bentonitized tuff band on a millimetric scale at all the outcrops, we observed that some bed contacts are gradational rather than sharp or erosional. Both normal and inverse grading is common, but the former is predominant. Many thick tuffaceous mudstone beds consist of various units distinguished by subtle colour

Figure 11. Field photograph showing small-scale trough cross-bedding, Khanpur section. The coin is 2.5 cm in diameter.

variation and in a few cases they are bounded by fine-grained laminated sandstones at the base and clay layers at the top. This colour and compositional layering may be caused by high-density currents and subsequent suspension settling according to the density and size of the particles.

2.b.1.b. Current reworked tuff facies Close to the delta front, beds are tens of centimetres thick and the sediments are relatively coarse-grained. They comprise several discrete depositional units, representing sediments driven by bottom currents. Many bentonitized tuff beds and tuffaceous mudstone facies are interstratified with these coarse-grained facies, indicating reworking and redistribution of ash by these bottom currents. Lenticular cross-bedded sandstone (Fig. 11) with abundant cross-lamination associated with tuffaceous mudstone facies indicates the influence of aqueous traction currents. Some of the bentonitized tuff and tuffaceous mudstone beds exhibit ripple cross-laminated units, and many of them are structureless units that contain sporadic small claystone intraclasts. Occasionally thin, very poorly sorted tuffaceous mudstone beds with subtle normal grading and sharp bases are present. This facies association is interpreted as debris flow-driven sedimentation. The presence of abundant small-scale climbing ripples and cross-lamination with 1.5 to 5 cm wavelengths indicates high rates of net deposition due to decelerating flows resulting from river floods or turbidity current (e.g. Allen, 1982). In the studied area the climbing ripples occur in association with thin sandstone layers which exhibit oscillation ripples (Fig. 7), indicating wave reworking of the unconsolidated bentonitized tuff in shallow-water settings. The tuffaceous mudstone beds exhibit considerable reworking and contamination from the enclosing claystones, siltstones and sandstones, and are interpreted as representing interfluvial settings. These deposits are laterally continuous for a few kilometres and are not associated with any major channel sand body. These facies associations are dominated by mottled mudstones characterized by rhizoids

Figure 12. Prograding lacustrine delta foresets embedded within the mudstone–siltstone units at Khanpur outcrop. Arrow indicates direction of progradation; hammer length is 30 cm.

Figure 13. Field photograph showing current-ripples, Bada Khetar section. The diameter of the scale is 6 cm.

and burrows (less developed soils), and lensoidal sandstones showing no lateral grain-size variation.

2.b.2. Pro-delta facies

The pro-delta facies sequence typically shows distinct coarsening-upward facies stacks ranging from silty, wavy bottomsets to sandy pro-delta foresets (Fig. 12). The pro-delta claystones, deposited below wave base from suspension, lack current-produced laminae, but are subtly graded or colour-banded due to slight differences in grain size or colour, related to discharge fluctuations. Bioturbation is intense in horizons produced during a period of decreased sedimentation rate. Towards the top of the sequence, parallel and lenticular silt laminae and thin cross-laminated sandstones are intercalated with claystones, suggesting the combined influence of waves, sediment-laden current incursion from the distributaries and deposition from suspension. In places, the pro-delta sediments are characterized by soft sediment deformation features. These features may be formed due to mass movement from the delta front. Because the very high sedimentation rate on the delta front does not allow pore fluids to escape during burial, high pore fluid pressure in uncompacted sediments leads to loss of sediment shear strength. Thus, the process of mass movement sets in, which leads to the development of deformational features. Pebble imbrication and climbing ripple lamination could be related to the frequent occurrence of strong downslope currents, probably during periods of river flooding. The basinward continuation of such flows may deposit a distinctive lacustrine pro-delta facies composed of interlaminated claystones, siltstones and very fine sandstones.

2.b.3. Delta front facies

The delta front sequence is composed of siltstones and fine- to medium-grained sandstones characterized by both wave and current ripples (Figs 7, 13). Bentonitized tuff beds exhibit prograding bed-sets which are characterized by calcretes (carbonate nodules, etc.) (Kamini section), various types of wave and current ripples (Uttar Behani section), rootlets, bioturbation and microflora and fauna (S. N. Kundal, unpub. data), reflecting deposition along the delta front in lacustrine conditions (e.g. Schäfer & Stapf, 1978). Lake slopes at some distance away from the river delta receive only fine-grained sediments from underflows. A delta front can become unstable due to oversteepening as well as overloading and result in sandy debris flows, causing slumps and convolution in the fine-grained slope sediments.

2.b.4. Deltaic distributary mouth-bar facies

The distributary mouth-bar facies comprises fine- to medium-grained sandstones. These sandstones are characterized by multidirectional planar and small-scale trough cross-beds. These planar and trough cross-bedded sandstones are lenticular in shape and rarely exhibit scour-and-fill structures and discontinuous claystone lenses/pebbles. The distributary channels are represented by large sandstone bedforms which are capped by a fining-upward sequence of fine-grained sediments deposited after distributary abandonment. In some places the upper parts of the coarsening-upward sequence are eroded by the distributary channels as a result of progradation. Away from the axis of the distributary, sandstones diminish and pro-delta claystones pass upward into interdistributary claystones and siltstones.

2.b.5. Interfluvial facies

Interfluvial areas in most of the fluvial basins are low-lying features showing development of floodplain, swamps and ponds (Singh *et al.* 1999). These typically low-lying areas with respect to the river channels are characterized by the facies architecture that indicates crevasse splay and suspended fall-out of fine-grained sedimentation. These deposits are usually referred to as overbank or flood plain deposits. Smith &

https://doi.org/10.1017/S0016756807003998 Published online by Cambridge University Press

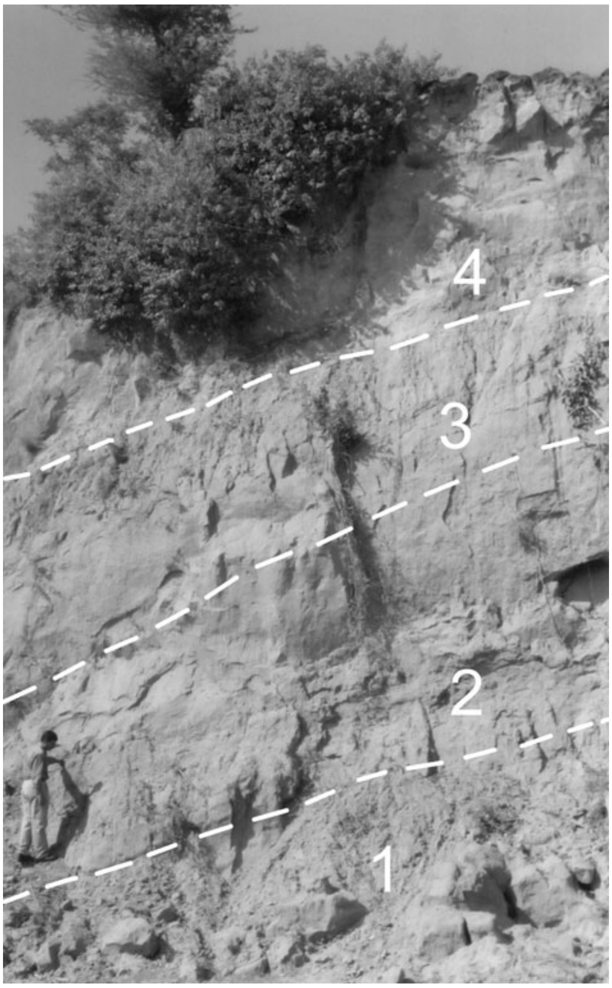

Figure 14. Succession of upland interfluvial facies, Khanpur section. 1 – laminated mudstone facies, 2 – siltstone facies, 3 – structureless mudstone facies and 4 – fine-grained sandstone facies. SKP standing on the outcrop is 1.70 m tall.

Perez-Arlucea (1994), Tye & Colman (1989*a*,*b*), Farrell (1987), Ray (1976), Singh (1972), Singh *et al.* (1999) and Sharma, Sharma & Singh (2001) have studied these deposits in modern environments and concluded that many of the thick mud-dominant fluvial deposits of the ancient fluvial record represent deposition in interfluvial areas. In some major alluvial plains (e.g. Ganga plain), the interfluvial areas include large tracts of deposition of muddy sediments located above the major channels and have been referred to as upland interfluve areas (Singh *et al.* 1999). Srivastava *et al.* (1994) and Kumar *et al.* (1996) have studied this type of muddy sediment in the Ganga plain, and Singh *et al.* (1999) have carried out a comparative study of these interfluvial deposits in Ganga plain and Lower Siwalik strata in Jammu. In our studied area, the interfluvial (upland area) facies consists of very fine-grained sandstones, laminated and structureless claystones (Fig. 14) deposited in the inter-channel areas. The brown and light yellow claystones and siltstones underlying the bentonitized tuff band are persistent over a few kilometres in all the measured sections. These claystones display thin (1–2 mm thick) wavy and parallel lamination, numerous dwelling burrows (2–5 mm in diameter) and minor organic debris. In some places, thickly bedded, finely laminated siltstones and claystones exhibit preserved rootlets and mottling. Interbedded with claystones are many thin (5–15 cm thick) beds of structureless, silt-bearing fine-grained sandstones. In some cases, mottling and secondary carbonate accumulations are observed. Similar sedimentary characters have been reported from the Dag section (Burbank & Tahirkheli, 1985) and Potwar Plateau (Visser & Johnson, 1978) from the coeval lithounits in Pakistan embedding a bentonitized tuff band and tuffaceous mudstones. The upper portion of the brown and light yellow claystones and siltstones yields a rich assemblage of microfossils, such as gastropods, bivalves, bone fragments, ostracodes, charophytes and angiosperm seeds from all the studied localities (Bhatia, Bhat & Pandita, 2001; S. N. Kundal, unpub. data) at this stratigraphic level. This micro-faunal and floral association is characteristic of shallow freshwater lakes.

The tuffs interbedded within interfluvial sediments, often cross-bedded, display both current- and toolmarks. Reworking is common, which is reflected by an abundant admixture of siliciclastic detritus in tuffaceous beds, and in some instances erosion of the entire tuff beds has taken place. These ash beds are affected by reworking to varying degrees to form mixed pyroclastic–siliciclastic beds, as are reported from the sections between Karju Tiba and Kherdi and other sections. The dominant mottled mudstone facies, with the presence of rootlets and bioturbation, is associated with thin lensoidal sand bodies, moderately to well sorted, which are persistent over a few kilometres without any marked change in grain size. These sandstone bodies do not merge laterally with any major channel sandstone bodies. The claystone facies is characterized by calcareous nodules and bedded calcretes. All of these sediment characters are typical of interfluvial depositional settings.

3. Stratigraphic significance

For description and correlation of the stratigraphy in basin analysis, lithology is the basic component to be studied, with fauna and flora providing additional constraints (if present in the sediments). As we begin to examine the rock record, we encounter a number of gaps in it and find the fauna and flora sporadically distributed in the continental sediments. In such cases, matching the sedimentary characters is the only way to correlate litho-sections. In addition, the distribution of fauna and flora in a basin provides spatio-temporal limits which aid in understanding the evolutionary history of a basin. However, fauna and flora have their own limitations, particularly when they are sporadically distributed. More accurate correlation in time is dependent on many available chronostratigraphic techniques. The accuracy of the chronostratigraphic correlation is directly related to the time-diagnostic criteria on which it is based (e.g. Prothero & Schwab, 1996). In the Siwalik basin, both litho- and biostratigraphic units tend to be localized in extent and the lithostratigraphic units are diachronous. This poses problems for the correlation of distantly placed lithostratigraphic units. Johnson *et al.* (1982) concluded that the age fluctuations on the order of 10^5 years might be anticipated for the Siwalik formations within a radius of 20 km of the designated stratotypes. During the last two decades, absolute chronological correlation of the Siwalik strata has been attempted by using magnetic polarity stratigraphy (e.g. Johnson *et al.* 1982; Azzaroli & Napoleone, 1982) and fission track dating techniques (Johnson *et al.* 1982; Ranga Rao *et al.* 1988). Johnson *et al.* (1982) have given a detailed account of the occurrence and fission track ages of the zircon phenocrysts from the bentonitized tuff band and tuffaceous mudstones in the Siwalik Group of Jhelum, Campbellpore and Chinji-Nagri areas in Pakistan. They have demarcated the boundary between the Tatrot and Pinjor faunal zones at 2.48 Ma, coincident with the Gauss–Matuyama transition. The bentonitized tuff and tuffaceous mudstone beds in two sections of our study (Khanpur (= Nagrota) and Bada Khetar) have been dated by Ranga Rao *et al.* (1988) using zircon fission track analysis at 2.31 ± 0.54 Ma and 2.8 ± 0.56 Ma, respectively. They calibrated the fission track ages of these bentonitized tuff and tuffaceous mudstone beds with magnetostratigraphy and biostratigraphy (vertebrate fauna) in these sections. The age determined by Ranga Rao *et al.* (1988), followed by Agarwal *et al.* (1993), and reaffirmed by Bhatia, Bhat & Pandita (2001), also coincides with the Gauss–Matuyama transition and marks the Tatrot–Pinjor boundary in the region. It is interesting to note that the first appearance datum of *Lychnothamnus barbatus* in the fossil state in Bada Khetar and Uttar Behani sections below the bentonitized tuff band (Bhatia, Bhat & Pandita, 2001) and in the intermontane basin of the Kashmir valley (as in the Hirpur Formation, Karewa Group) is synchronous, namely late Pliocene, below the volcanic ash bed dated at 2.4 ± 0.4 Ma (see Bhatia, Soulie-Marsche & Gemayel, 1998). Our study reveals that the persistent nature of this conspicuous, geographically widespread single ash bed (bentonitized tuff band and tuffaceous mudstones) traced for about 45 km along-strike (Fig. 1), whose outcrops are further traceable in the region, within its area of occurrence is an invaluable time-marker horizon.

4. Discussion

Acidic volcanic ashes were deposited as distal pyroclastic fallout in the northwestern part of the Siwalik basin during late Pliocene times. The Dacht-e-Nawar volcanic complex of East-Central Afghanistan (about 1000 km to the northwest of the study area) has been projected as its probable source (Johnson *et al.* 1982). The ash falls normally exhibit either density- or size-graded bedding, however, the depositing medium and the endogenous processes are likely to control the mode of preservation as well. The volcanic ash deposits under discussion represent one such example, where the mode of preservation was influenced by the upland interfluvial–lacustrine processes. We recognized three distinct depositional settings in these interfluvial–lacustrine depositional domains with varying preservation potential of the bentonitized tuff and tuffaceous mudstones. These depositional settings include: (1) central plains of the lakes, (2) shoreline and delta fronts of these lakes, and (3) interchannel areas. The central plain lacustrine setting is the best preservation domain for ash falls interbedded with lacustrine claystones. In this sedimentation domain, the pure and thick bentonitized tuff beds displaying sharp basal contacts, followed upwards by distinct phases distinguished by change in colour, texture, grading and thickness, represent primary ash-fall phases in calm areas of the lake. These bentonitized tuff beds show laterally constant thickness over hundreds of metres. In the graded beds, coarseness and bed thickness are positively correlated and are interpreted as characteristic of lacustrine settings (e.g. Reineck, 1974; Allen, 1982). Wind-driven surface currents can be very effective in distributing suspended sediment, especially during ash falls which may have minimized the density contrast between river inflow and lake water (e.g. Weirich, 1986). These processes are likely to generate rhythmic sequences ranging from sandy, mostly thin-bedded proximal bottomsets (Fig. 9b1) to varve-type distal rhythmites (Fig. 9b2). The presence of ash rhythmites, good sorting and normal grading in bentonitized tuff beds also indicates primary ash-fall settling in low-energy lacustrine settings. The good preservation of rhythmites points to a high sedimentation rate in oxic bottom conditions, minimal bottom current activity and a relatively extensive flat floor below wave base, and minimum biogenic gas bubble generation. Lake slopes at some distance away from river deltas receive only fine-grained material from wind-driven overflows. Additionally, lake shores are little influenced by river inflow and exhibit a transitional stage between oversupplied and sediment-starved conditions. Under these conditions lacustrine flora flourishes on the lake slopes which receive little sediment (fine-grained) from the upland region during rainy seasons (Fig. 9a). Some of these fine-grained slope sediments are transported by slumps and debris flows into the deeper lake. In these settings, seasonally driven silt and clay layers are thinner and finer grained and the deposits of individual flow events may not be distinguishable (e.g. Ashley, 1975; Sturm & Matter, 1978).

Thin parallel lamination (subtly density- and size-graded, and devoid of escape burrows) in bentonitized tuff beds results from settling, through a still water column, of ash particles spread over the lake surface by pyroclastic fall (e.g. Anderson, Nuhfer & Dean, 1985; Nelson *et al.* 1986). Reverse grading, as observed

https://doi.org/10.1017/S0016756807003998 Published online by Cambridge University Press

in our study (Tawi River section), may have been caused by such a mechanism (e.g. Self, 1976). The ferromagnesian high density minerals (specific gravity ranging from 3.1 to 4.7) settled more quickly than the felsic minerals (density ranging from 2.5 to 2.6) on the lake bottom, forming density- and size-graded laminae. The light coarser fraction and flaky minerals (biotite) were held in suspension for a relatively longer time than the high density fraction, leading to the formation of reverse grading. The bentonitized tuff band sequence is conspicuous in all of the four inferred lake basins with its best development in the Mandal-Uttar Behani area. Bhatia, Bhat & Pandita (2001) recovered a microfossil assemblage from the underlying claystone units at these localities consisting of ostracodes, charophyte gyrogonites and angiosperm seeds, which suggests a depth range varying from a minimum of 2 m at Uttar Behani to a maximum of 6 m at Bada Khetar. Facies architecture and sedimentary structures observed in the bentonitized tuff beds and the underlying claystones also indicate deeper settings at the Bada Khetar locality, which progressively decreases on either side towards Uttar Behani and Mandal over a distance of about 3 km. The same microfaunal and microfloral assemblages recovered from the Khanpur–Kamini, Kherdi–Anandpur and Dora–Karju *Tiba* areas (S. N. Kundal, unpub. data) also suggest similar depositional settings for these inferred lake basins.

The shoreline and deltaic facies represent pro-delta, sand-rich mouth-bar, and small-scale distributary channel subenvironments. Dispersion of river water into the lakes commonly varies according to season. Sediment-laden underflows are evidently common events, capable of rapidly introducing large volumes of suspended sediments to the bottom of many lakes (e.g. Weirich, 1986). In humid tropical and sub-tropical lakes, sediment-laden underflows commonly persist throughout the year because of continuous sediment supply (e.g. Tiercelin *et al.* 1992), resulting in density contrast between the river and lake waters. Because of the greater density contrast, muddy flood waters plunge abruptly beneath the clear lake waters within a very short distance of the river mouth bars. The underflows (hyperpycnal flows: see Bates, 1953) may produce sublacustrine channels and levees. Large sediment-laden underflows can cause lacustrine deltas to prograde rapidly over finer-grained, pro-delta deposits. This process may lead to reworking of unconsolidated ashes and form erosionally based climbing ripple- and planar-bedded graded bentonitized tuff and tuffaceous mudstone beds with load casts at their bases. Liquefaction and load structures result, because of the density instability in this type of depositional setting. The rapid accumulation of sediments and steep accretionary foresets also induces slope instability and provides a source for sandy debris flows. The interbedded lenticular sandstone and tuff layers showing reverse grading, basal scours, imbricated planar clasts and rafted mudstone clasts are typical of sandy debris flows (e.g. Shanmugam *et al.* 1995; Shanmugam & Moiola, 1995; Shanmugam, 2002, 2003). The ripples and sand bars preserved beneath these lacustrine deposits reflect rapid but low-energy flooding events within the basin. Sediments deposited near the bar crests are characterized by relatively well-sorted sandstones with cross-lamination, climbing ripple lamination and some flat lamination, deposited principally during river floods (e.g. Reading, 1996). These flooding surfaces are traceable for many kilometres along-strike. Lake slopes at some distance away from river deltas receive only fine-grained material from overflows. Some of these fine-grained slope sediments are transported by slumps and debris flows into the deeper parts of the lake. Load and flame structures observed in this study reflect pockets of dark, dense ash (ferromagnesian) bulging downward into the light ash layers (felsic), which in turn project upward in sharp diapir-like shapes drawn out into long streaks (flames). These flames, similar to those observed by Sorby (1908) from the Borrowdale Volcanic Series of the English Lake District, lean markedly from the vertical (Fig. 6), in the direction which is most probably that of the palaeoslope of the lake. The bentonitized tuff beds exhibiting prograding bed-sets characterized by carbonate nodules (Kamini section), various types of wave and current ripples (Uttar Behani section), rootlets, bioturbation and microflora and microfauna (S. N. Kundal, unpub. data) reflect deposition along the shoreline and delta front in lacustrine conditions (e.g. Schäfer & Stapf, 1978).

Tuffs interbedded within interfluvially driven sediments, often cross-laminated fine- to medium-grained sandstones, display both current- and tool-marks. Reworking is common and associated with an abundant admixture of siliciclastic detritus or erosion of the entire tuff beds. These ash beds are affected by reworking to varying degrees to form mixed pyroclastic–siliciclastic beds, as are reported from the sections between Karju Tiba and Kherdi and the sections between the four inferred lake basins. The dominant mottled mud facies, virtually devoid of any organic matter, is associated with thin, moderately to well-sorted, lensoidal sand bodies. These sand bodies are persistent over a few kilometres without any change in grain size. This mudstone–sandstone facies association has been deposited in upland interfluvial depositional settings (e.g. Sharma, Sharma & Singh, 2001). The mud facies is characterized by calcareous nodules and bedded calcretes. The minor floral debris present in these sediments may have been derived from shallow zones of the ponds. Bulk chemical composition of the bentonitized tuff beds, with pH varying from 7.8 to 8.4, reveals markedly high Mg and K values and depleted Si, Ca, Na, Al and Fe values (Bhat & Pandita, 1998). These variations are related to the effect of secondary Mg and K gain and Si, Fe, Ca and Na loss during the depositional phase in lakes rich in Mg and K. Similar trends observed in thoroughly altered ash layers have been related to the reaction of ash fall within sea water, resulting in Na loss and K gain (Jezek & Noble, 1978). The lakes receiving sediments at a high rate have a short life span, and pro-delta and proximal bottom sediments make up the bulk of their sediment fill, as appears to be the case in the present study. This sediment fill typically shows a distinct coarsening-upward sequence from silty, varve-type bottomsets to sandy pro-delta foresets and fluvial sand and gravel.

5. Conclusions

(1) A conspicuous and geographically widespread bentonitized tuff band and tuffaceous mudstones of late Pliocene age occur in the Nagrota B Member of the Upper Siwalik Subgroup. We have established continuity of this bentonitized tuff and the tuffaceous mudstone beds along-strike for about 45 km in the region. These beds represent an important time-marker horizon within their area of occurrence, which coincides with the Gauss–Matuyama transition at 2.48 Ma. The bentonitized tuff and tuffaceous mudstones provide tools for correlation of the laterally diachronous fluvial strata in the northwestern part of the Siwalik basin.

(2) The bentonitized tuff and tuffaceous mudstone beds, and the under- and overlying strata, exhibit laterally varying facies architecture representing upland interfluvial–lacustrine depositional domains. This sequence typically shows distinct coarsening-upward facies stacks, ranging from silty, wave-type bottomsets to sandy pro-delta foresets, and mouth-bar facies capped by fluvial sandstones and gravels. The lateral stacks of these facies within the measured sections are related to the chain of four lake basins; all of them document bentonitized tuff and tuffaceous mudstone beds.

(3) In these lakes, three distinct depositional settings with different preservation modes for the bentonitized tuff and tuffaceous mudstones have been recognized. They include (1) the central plain of the lake, (2) shoreline and delta fronts, and (3) inter-channel areas. Among these, the central plain lacustrine settings exhibit the best record of both primary and reworked ash falls.

Acknowledgements. We gratefully acknowledge the help extended by Prof. Dorrik A. V. Stow, University of Southampton, in describing the structures in bentonitized tuff band. Constructive criticism offered by Prof. G. Shanmugam and two anonymous referees helped us in improving the manuscript in many ways. We appreciate help rendered by Mr Vinay Sharma in making computer graphics for the paper. SNK acknowledges the L. Rama Rao birth centenary grant for the year 2000–2001 from the Geological Society of India, Bangalore.

References

Agarwal, R. P., Nanda, A. C., Prasad, D. N. & Dey, D. K. 1993. Geology and biostratigraphy of the Upper Siwalik of Samba area, Jammu foothills. *Journal Himalayan Geology* **4**, 227–36.

Allen, J. R. L. 1982. *Sedimentary Structures: Their Character and Physical Basis. Developments in Sedimentology*. Amsterdam, New York, Oxford: Elsevier Science Publishing Company, 663 pp.

Anderson, R. Y., Nuhfer, E. B. & Dean, W. E. 1985. Sedimentation in a blastzone lake at Mount St. Helens, Washington – Implications for varve formation. *Geology* **13**, 348–52.

Ashley, G. M. 1975. Rhythmic sedimentation in glacial Lake Hitchcock, Massachusetts–Connecticut. In *Glaciofluvial and Glaciolacustrine sedimentation* (eds A. V. Jopling & B. C. MacDonald), pp. 304–20. Society of Economic Palaeontologists and Mineralogists, Special Publication no. 23.

Azzaroli, A. & Napoleone, G. 1982. Magnetostratigraphic investigations of the Upper Siwalik near Pinjor, India. *Revista Italiana Palaeontologia* **87**, 739–62.

Bates, C. C. 1953. Rational theory of delta formation. *American Association of Petroleum Geologists Bulletin* **37**, 2119–62.

Bhat, G. M. & Pandita, S. K. 1998. Sedimentology, mineralogy and geochemistry of fallout tephra deposits in Upper Siwalik Subgroup, Jammu, India. 13th Himalaya–Karakoram–Tibet International Workshop. Special Issue, *Geological Bulletin, University of Peshawar* **31**, 34–6.

Bhat, G. M., Pandita, S. K., Singh, R., Malik, M. A. & Sarkar, S. 1999. *Northwest Himalayan Successions along Jammu–Srinagar Transect (Field Guide)*. Indian Association of Sedimentologists, Aligarh, India, 141 pp.

Bhatia, S. B., Bhat, G. M. & Pandita, S. K. 2001. Microfossils from the Nagrota Formation, Upper Siwalik Subgroup, Jammu Hills. *Journal Geological Society of India* **58**, 509–18.

Bhatia, S. B., Soulie-Marsche, I. & Gemayel, P. 1998. Late Pliocene and early Pleistocene charophyte flora of the Hirpur Formation, Karewa Group, Kashmir, India. *Neues Jahrbuch für Geologie und Paläontologie, Abhandlungen* **210**, 185–209.

Burbank, D. W. & Tahirkheli, R. A. K. 1985. The magnetostratigraphy, fission track dating, and stratigraphic evolution of the Peshawar intermontane basin, northern Pakistan. *Geological Society of America Bulletin* **96**, 539–52.

Farrell, K. M. 1987. Sedimentology and facies architecture of overbank deposits of the Mississippi River, False River region, Louisiana. In *Recent Development in Fluvial Sedimentology* (eds F. G. Ethridge, R. M. Flores & M. D. Harvey), pp. 111–20. Society of Economic Palaeontologists and Mineralogists, Special Publication no. 39.

Fisher, R. V. & Schmincke, H. U. 1984. *Pyroclastic Rocks*. Heidelberg, New York: Springer-Verlag, 472 pp.

Gupta, S. S. & Verma, B. C. 1988. Stratigraphy and vertebrate fauna of the Siwalik Group, Mansar–Uttarbani section, Jammu district, J & K. *Journal of the Palaeontological Society of India* **33**, 117–24.

Jezek, P. A. & Noble, D. C. 1978. Natural hydration and ion exchange of obsidian: an electron microprobe study. *American Mineralogist* **63**, 266–73.

Johnson, G. D., Zeitler, P., Naeser, C. W., Johnson, N. M., Summers, D. M. & Frost, C. D. 1982. The occurrence and fission track ages of late Neogene and Quaternary volcanic sediments, Siwalik Group Northern Pakistan. *Palaegeography, Palaeoclimatology, Palaeoecology* **37**, 63–93.

Kumar, S., Parkash, B., Manchanda, M. L., Singvi, A. K. & Srivastava, P. 1996. Holocene landform and soil evolution of the western Gangetic Plains: Implications of neotectonics and climate. *Zeitschrift für Geomorphology*, special edition, **103**, 283–312.

Nelson, C. H., Meyer, A. W., Thor, D. & Larson, M. 1986. Crater Lake, Oregon: a restricted basin with base-of-slope aprons of non-channellized turbidites. *Geology* **14**, 238–41.

Prothero, D. R. & Schwab, F. 1996. *Sedimentary Geology: An Introduction to Sedimentary Rocks*. Freeman, 575 pp.

Ranga Rao, A., Agarwal, R. P., Sharma, U. N., Bhalla, M. S. & Nanda, A. C. 1988. Magnetic polarity stratigraphy and vertebrate palaeontology of the Upper Siwalik Subgroup of Jammu hills, India. *Journal of the Geological Society of India* **31**, 361–5.

Ray, P. 1976. Structure and sedimentological history of the overbank deposits of a Mississippi River point bar. *Journal of Sedimentary Petrology* **46**, 788–801.

Reading, H. G. 1996. *Sedimentary Environments: Processes, Facies and Stratigraphy*. London: Blackwell Science, 688 pp.

Reineck, H. E. 1974. Schichtgefüge der Ablagerungen im tieferen Seebecken des Bodensees. *Senckenbergiana Maritima* **6**, 47–63.

Schäfer, A. & Stapf, K. R. G. 1978. Permian Saar-Nahe Basin and Recent Lake Constance (Germany): two environments of lacustrine algal carbonates. In *Modern and Ancient Lake Sediments* (eds A. Matter & M. E. Tucker), pp. 83–107. International Association of Sedimentologists, Special Publication no. 2.

Self, S. 1976. The recent volcanology of Terceira, Azores. *Journal of the Geological Society, London* **132**, 645–66.

Shanmugam, G. 2002. Ten turbidite myths. *Earth-Science Reviews* **58**, 311–41.

Shanmugam, G. 2003. Deep-marine tidal bottom currents and their reworked sands in modern and ancient submarine canyons. *Marine and Petroleum Geology* **20**, 471–91.

Shanmugam, G., Hermance, W. E., Olaifa, J. O. & Odior, E. G. 1995. Slump dominated upper slope reservoir facies, Intra Qua Iboe (Pliocene), Edop Field, offshore Nigeria. *American Association of Petroleum Geologists Annual Convention Official Program, 88A*, abstract.

Shanmugam, G. & Moiola, R. J. 1995. Reinterpretation of depositional processes in a clastic flysch sequence (Pennsylvanian Jackfork Group), Ouachita Mountains, Arkansas and Oklahoma. *American Association of Petroleum Geologists Bulletin* **79**, 672–95.

Sharma, S., Sharma, M. & Singh, I. B. 2001. Facies characteristics and cyclicity of Lower Siwalik sediments, Jammu area: a new perspective. *Geological Magazine* **138**, 455–70.

Singh, I. B. 1972. On the bedding in the natural levee and the point bar deposits of the Gomti River, Uttar Pardesh, India. *Sedimentary Geology* **7**, 309–17.

Singh, I. B., Srivastava, P., Sharma, S., Sharma, M., Singh, D. S. & Rajagopalan, G. 1999. Upland interfluve (Doab) deposition: alternative model to muddy overbank deposits. *Facies* **40**, 197–210.

Smith, N. D. & Perez-Arlucea, M. 1994. Fine-grained splay deposition in the avulsion belt of the Lower Saskatchewan River, Canada. *Journal of Sedimentary Research* **64**, 159–68.

Sorby, H. C. 1908. On the application of quantitative methods to the study of the structure and history of rocks. *Quaternary Journal of the Geological Society of London* **64**, 171–267.

Srivastava, P., Parkash, B., Sehgal, J. L. & Kumar, S. 1994. Role of neotectonics and climate in development of the Holocene geomorphology and soils of the Gangetic Plains between the Ramganga and Rapti rivers. *Sedimentary Geology* **94**, 129–51.

Sturm, M. & Matter, A. 1978. Turbidites and Varves in Lake Brienz (Switzerland): deposition of clastic detritus by density currents. In *Modern and Ancient Lake Sediments* (eds A. Matter & M. E. Tucker), pp. 147–68. International Association of Sedimentologists, Special Publication no. 2.

Tandon, S. K. & Kumar, R. 1984. Discovery of tuffaceous mudstones in the Pinjor Formation of Panjab Sub-Himalaya, India. *Current Science* **53**(18), 982–4.

Tiercelin, J. J., Soreghan, M., Cohen, A. S., Lezzar, K. E. & Bouroullec, J. L. 1992. Sedimentation in large rift lakes: example from the Middle Pleistocene–Modern deposits of the Tanganyika trough, East African rift system. *Bulletin Centre de Recherches Exploration Production Elf-Aquitaine* **16**, 83–111.

Tye, R. S. & Coleman, J. M. 1989*a*. Depositional processes and stratigraphy of fluvially dominated lacustrine deltas: Mississippi Delta Plain. *Journal of Sedimentary Petrology* **59**, 973–6.

Tye, R. S. & Coleman, J. M. 1989*b*. Evolution of Atchafalaya lacustrine deltas, South-Central Louisiana. *Sedimentary Geology* **65**, 95–112.

Visser, C. F. & Johnson, G. D. 1978. Tectonic control of late Pliocence molasses sedimentation in a portion of the Jhelum re-entrant Pakistan. *Sonderdruck aus der Geologischen Rundschau* **67**, 15–37.

Weirich, F. H. 1986. A study of the nature and incidence of density currents in a shallow glacial lake. *Annals of the Association of American Geographers* **76**, 396–413.